Imaging of ferroelectric micro-domains in X-cut lithium niobate by confocal second harmonic microscopy

GERHARD BERTH,[1] VOLKER WIEDEMEIER, KLAUS-PETER HÜSCH,
LI GUI, HUI HU, WOLFGANG SOHLER AND ARTUR ZRENNER

Department Physik, Universität Paderborn, Warburger Str. 100, D-33098 Paderborn, Germany

We present results on ferroelectric micro-domains obtained by confocal second harmonic microscopy. The high potential of this technique is demonstrated by imaging periodic ferroelectric domain structures in the surface of planar X-cut lithium niobate (LN) and in the body of ridges fabricated by plasma etching on X-cut LN as well. In both cases the measured second harmonic signal reveals a strong contrast between inverted and non-inverted domain sections. This enabled a depth-resolved non-destructive tomography of micro-domains in ridge structures in all three dimensions.

Keywords: Nonlinear microscopy, ferroelectric micro-domains, confocal imaging, LiNbO$_3$

1. INTRODUCTION

Second harmonic microscopy has become an invaluable tool in the field of diagnostics and basic research [1,2,3]. In the confocal mode, this technique enables a high spatial resolution in three dimensions for advanced image acquisition [4]. Amongst other methods the second harmonic microscopy enables investigations of ferroelectric domain structures [5]. Ferroelectrics, e.g. lithium niobate (LN), play a significant role in the field of integrated optics. Here periodically poled waveguides are required to get quasi-phase matched (QPM) nonlinear interactions for applications in the area of frequency conversion (e.g. second harmonic, sum- and difference-frequency generation (SHG, SFG, DFG), optical parametric amplification and oscillation (OPA, OPO)) [6,7]. Periodically poled X-cut devices are of particular interest for specific devices such as high-speed band pass modulators [8]. Ferroelectrics are also promising materials for the

---

[1] Corresponding author. E-mail: berth@physik.upb.de

development of photonic nanowires, where also QPM is needed for second order nonlinear processes [9]. In this context investigations of ridge waveguides will be helpful for their development.

Crucial for high quality nonlinear optical devices is the control of domain fabrication. In our work we investigate the periodic micro-domain structures in the surface of planar X-cut LN and in the body of plasma-etched ridges on X-cut LN. The domain structures were fabricated by electric field assisted poling using periodic micro-electrodes. Nonlinear confocal laser scanning microscopy (CLSM) was used to investigate the micro-domains. This method allows a direct and non invasive study of the domain structures with high resolution in three dimensions [10].

2. CONFOCAL SHG MICROSCOPE

We have developed a modular setup based on the confocal laser scanning technique. Generally, operation in a linear optical or a nonlinear mode is feasible with detection channels in reflection and transmission geometry. Measurements presented in this contribution have been done in the backward direction (reflection). The confocal microscope is schematically depicted in figure 1; it was realized with "infinity-corrected" objectives. In this special configuration the incoming laser beam is focused by an infinity-corrected microscope objective to a diffraction-limited spot. The signal to be detected is focused likewise by a detector lens onto the confocal pinhole. In contrast to the standard configuration this setup offers a high degree of flexibility in the system design as collimated beams are not affected by the insertion or removal of (plane) optical components like filters or polarizers. Two infinity-corrected microscope objectives (O1: N-Plan 100x/0.9/0.27, O2: PL-Fl-L 100x/0.75/4.7) are implemented for focussing the incoming laser beam and for collecting the light to be detected respectively. A pinhole placed in front of the detector is responsible for the confocal characteristic of the system [11]. For our measurements we typically used a pinhole of 2 µm diameter. Information, which does not originate from the focal plane of the microscope objective, is faded out by this arrangement. In contrast, light from the focal plane is focused on the pinhole and passes to the detector. The advantage of out-fading information from above or below the focal plane enables the confocal microscope to perform depth-resolved measurements. Image acquisition is accomplished by scanning the sample with a nano-positioner under the condition of a spatially fixed laser focus. In the confocal mode a genuine 3D-image can be processed by scanning of sequential levels. A complex system of positioning-units allows inspection areas up to

5" x 5" in size. The adjustment of the optical system (pinhole modules, objectives, intermediate imaging, fiber-coupling, etc.) is driven by piezo-actuators, which are realized as piezoelectric inertial-drives. Two display-units (LED, CCD, beam splitter) are used for conventional microscopy.

For linear measurements a Ti:sapphire laser (780 nm $<\lambda<$ 820 nm) operating in the continuous wave mode as well as a 100 mW diode pumped solid state laser (DPSSL) with an emission wavelength of 473 nm are available. By using the DPSSL the lateral resolution was determined to be $d_L \sim$ 300 nm by measurements on calibration structures and the axial resolution to $d_A \sim$ 500 nm via the FWHM-criterion.

For applications in second harmonic microscopy we use a 20 fs mode-locked Ti:sapphire laser (Femtosource C-20) pumped by a frequency doubled Nd:YVO$_4$ laser. The Ti:sapphire laser with an average output power of 500 mW at a centre wavelength of 800 nm emits pulses with a repetition rate of 80 MHz. We determined the pulse width of the excitation light in front of the objective to be $\sim$ 100 fs by an autocorrelation setup and the average power to be 100 mW. Under these conditions we obtain a peak pulse power density of about 1×10^{12} W/cm^2. For the spectral separation of the fundamental and the frequency-doubled signal dichroic beam splitters (FS 101495) and additional colour bandpass filters (BG39) were placed in the detection path. The frequency-doubled signal was detected by single photon counters based on avalanche photodiode modules. A Glan-Thomson-prism was used for polarization analysis. Using this setup we have performed investigations of periodic ferroelectric micro-domains in the surface of X-cut LN and in the body of ridges on X-cut LN.

3. MICRO-DOMAIN FABRICATION

The ridges were fabricated by inductively coupled plasma (ICP) etching [12]. Therefore a chromium film (220 nm) was deposited on the –X face of LN by a sputtering process. The Cr-mask for ICP etching was produced photolithographically (e-beam writing and wet chemical etching) resulting in defined Cr-stripes of 10 µm width. Etching (etching gas: C$_4$F$_8$/He-mixture) yielded ridge structures with heights between 2 and 3 µm. The remaining Cr stripe was removed by a cerium sulphate solution. Variation of the Cr stripe geometry enabled the fabrication of ridges of different size with heights up to $\sim$ 6 µm and widths of 4 µm. Figure 2 shows a SEM micrograph of such a ridge on X-cut LN.

Comb like electrodes were used for electric field assisted poling of the micro-domain structure. For electrode fabrication we have used lift-off lithography of a vacuum-deposited titanium layer (100 nm). Figure 2 shows schematics of the poling configuration for a planar X-cut (figure 3a) and a ridge LN sample (figure 3b). In both cases the electrode period was 16.6 µm with gaps of 8 to 14 µm between opposite electrodes. The indicated coordinate system corresponds to the crystallographic axes. For ridge samples electrodes are placed on the Z-faces of the ridge to confine the micro-domains to the body of the ridge. Poling has been performed in an oil bath to obtain a high isolation between two opposite electrodes with various types of high voltage pulses. We present results for poling with a series of rectangular pulses. The current/charge behavior during poling does not show an evident difference between planar and ridge samples. For different electrode gaps the pulse voltage level varies between 250 V and 550 V. The standard pulse duration is 10 ms and the time interval between consecutive pulses is 100 ms. Like in previous work [13] the largest charge flow was observed during the first pulse, decreasing fast with increasing pulse number, and saturating at a certain level after five pulses.

4. RESULTS AND DISCUSSION

Differently processed planar and ridge specimens with periodic micro-domains have been investigated to analyze the domain structures. By inspection via linear optical microscopy no observable surface damage on the X-face was found. For a more detailed analysis selective chemical etching, CLSM, and confocal nonlinear (second harmonic) scanning microscopy have been employed. For nonlinear measurements the polarization of the pump light was oriented parallel to the crystallographic Z-axis, where the highest nonlinear coefficient d_{33} is available.

Two typical SH images from the X-faces of planar X-cut samples with periodic micro-domains in the surface are shown in figure 4. The Ti-electrodes used for poling can be seen as well. The pulse durations for electric field assisted poling were 5 ms (figure 4a) and 20 ms (figure 4b).

We find enhanced SH signals from the areas between the electrodes, which represent domains of finite depth. A periodic pattern with a strong contrast between differently poled domains is observed, where an average 50:50 duty cycle becomes apparent. From these nonlinear data one can speculate that poling starts from the positive electrode and then grows towards the negative one. Also around (and under – see below) the positive electrode a nonlinear signal can be seen resulting from corresponding domain extension. For the inverted domains a stronger nonlinear

4

response and a more homogenous SH distribution is obtained by increasing the pulse duration. Moreover we observed an increasing area of enhanced nonlinear signal next to the positive electrodes.

From previous measurements on bulk Z-cut PPLN structures it is known, that the nonlinear signal from domain walls in the surface region is reduced with respect to the domain signal, whereas inside the crystal the opposite is observed [10,14]. Only in Ti: PPLN the surface signal from the walls is also enhanced [10]. Because of the absence of Ti or other doping components in the samples discussed in this contribution we did not expect such a SH signature in the surface region. In contrast to bulk PPLN the areas between the electrodes represent domain regions of finite depth (several micrometers). Based on these facts we suppose that the enhanced nonlinear response results from ensembles of buried micro-domains (see also below). In previous work a filamentation of poled domains, consisting of needle-like inverted filaments was only observed in Ti-doped samples [4, 13]. Here, besides the absence of Ti, also the poling conditions are quite different. Depending on the poling parameters a different fragmentation of the inner domain structure was observed. Resulting SH-images should depend on number, size, length and shape of the inner domain fragments. For the planar samples depth resolved analysis exhibits a confined depth expansion of the inverted domains of about 1 µm.

After this nonlinear analysis the samples were etched in HF: HNO_3 at room temperature for 20 minutes and imaged by optical microscopy. Here we observed regularly oriented scratch-like mark patterns in the areas where positive electrodes have been removed (etch depth ~ 200 nm). One possible explanation is that the application of high voltage has damaged surface parts under the positive electrodes, which are more easily etched.

In the following we present and discuss our results on ridge structures. For analysis with conventional microscopy and linear imaging via CLSM plasma-etched ridge samples have been selectively etched with HF:HNO_3 for 20 minutes. Here the etch just attacks the –Z-faces of the ridge and consequently transforms the domain structure to the surface topology. Since the side walls of the ridges are originally +Z and –Z-face, a periodical etch pattern can be seen on the top of the ridge as shown in the optical micrograph (figure 5a). Sometimes scratch-like patterns become visible under the region of the positive electrodes (figure 5b).

In the ridges nonlinear signatures are observed which are very similar to those of planar structures. Here also a strong second harmonic signal from the generated micro-domains was detected. The linear and the corresponding nonlinear image of a periodically poled ridge on X-cut LN are shown in figure 6 (laser focus on the level of the top face of the ridge). In the image taken with the linear mode of the microscope (figure 6 a) a periodic modulation of the side walls of the ridge, due to selective etching, is only indicated along the ridge edges (Z-faces). In contrast to the sample in figure 5a, this one has been etched for a shorter time, so the modulation just becomes visible in form of periodic tiny tips and dips at the domain boundaries. In the nonlinear image a periodic structure with a strong contrast becomes visible with the SH-intensity increased in the areas of successful domain inversion (figure 6 b). As for the surface domains we suppose that the nonlinear signal is induced by the inverted domain filaments or fragments embedded under the surface. It is known that the investigation of different poling states (different pulse duration etc.) by imaging the corresponding cross sections yields detailed information about the domain evolution [15]. So the existence of such a fragmentation inside the poled area was proved by analyzing the cross section of a periodically poled ridge (figure 7), which has been cut and polished along the direction indicated in the inset of the figure. A micrograph, taken from the original +Z-face of the ridge after chemical etching is shown in figure 7. It is obvious that for this sample poling has not been completed. The micrograph of the cross section of the periodically poled ridge shows differently segmented embedded domains. We suppose that this segmentation is responsible for the spatial intensity distribution of the SH signature. We can observe changes of the fragmentation of the inverted regions in Z-direction along the ridge (evolution in Z-direction).

In contrast to planar samples, the depth of inverted domains in poled ridges can grow up to ~ 5 µm. Two SH- images of ridge-surfaces and corresponding micrographs of cross sections from similar ridges are presented in figure 8. Please note that the depicted surface and corresponding cross section data have been obtained from similar but not identical ridge sections. Here also the cutting lines are indicated as dashed lines. The micrographs of the ridge surface exhibit a strong SH-contrast for oppositely poled areas. A comparison of the two samples shows that in the case of the specimen poled with 550 V the contrast between the poled and original structure is enhanced by a factor 2, while the contrast of ground (bulk) and ridge level is the same. Concerning the confocal mode the different levels of ridge and bulk material are visible (laser focused on the top of the ridge) also as a contrast in the nonlinear signal. The poled area appears as spatially extended

region from which the SH is generated. A hexagon-shaped cross section of the poled region becomes obvious for some poling conditions.

A more detailed analysis of the cross section (linear) images taken after selective chemical etching shows domain fragments inside or at the boundaries of the poled regions. The average cross section of the poled regions decreases from the +Z towards the –Z side of the ridge. This means that the number and/or the size of the domain fragments and/or the distance between them changes across the ridge. This also means that domain fragments may merge depending on the poling parameters. We suppose that all geometric changes in three dimensions enormously affect the spatial distribution of the SH-signatures of the poled regions.

We have also studied the nonlinear response as function of the depth inside the ridge by imaging a cross section in the confocal X/Y-plane. The result of such a measurement is shown in figure 9 including a schematic of the scan geometry. The scan increment was set to be 250 nm in X- and Y-directions. Such a scan geometry allows to observe the nonlinear properties of the ridge in a cross section without cutting the sample and without preferential etching. The different domains become clearly visible. Inside the inverted areas an inner modulation of the SH-signal is still observable evidence for the existence of embedded domain fragments. Furthermore, the average shape of the poled areas appears as a hexagonal structure, which corresponds to preferential crystallographic orientations.

The result of a SH-tomography of the poled ridge structure is given as a sequence of 5 confocal images originating from planes of different depths (figure 10). The upper scan depth was chosen to be the top surface of the ridge ($d_x = 0$ µm). The maximum depth of the inverted regions was determined to be ~5 µm. In all images a contrast in SH intensity between areas of opposite domain orientation is clearly visible. The diminution in +Z-direction of the areas with strong SH-signature can also be seen. Due to different depth positions of the focal plane, the contrast between the nonlinear signal from the non-inverted areas inside the ridge and from the bulk material changes. It can also be seen, that the areas underneath the positive poling electrodes (removed) are strongly poled next to the ridge.

5. CONCLUSION

Confocal second harmonic microscopy has been employed for a depth resolved investigation of periodic ferroelectric micro-domains in the surface of X-cut LN and in ridges fabricated by ICP-

etching on X-cut LN. The results show that an electric field assisted poling of ridge structures via comb like electrodes can be successfully performed. A detailed analysis has revealed the existence of domain fragments inside the poled areas, which can vary significantly also dependent on the fabrication parameters. At the moment we can only speculate why such a high nonlinear signal arises from the embedded micro-fragments of ferroelectric domains. Therefore, more systematic investigations of this phenomenon and theoretical modelling will be necessary.

ACKNOWLEDGMENT

Figures:

Figure 1 G. Berth et al., Ferroelectrics
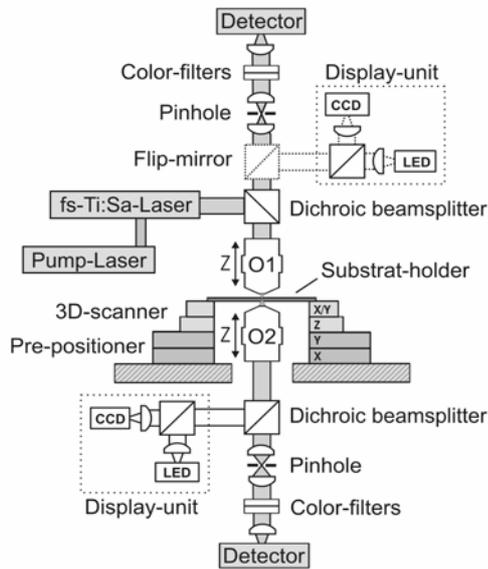
Figure 2 G. Berth et al., Ferroelectrics
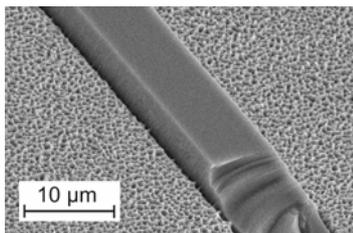
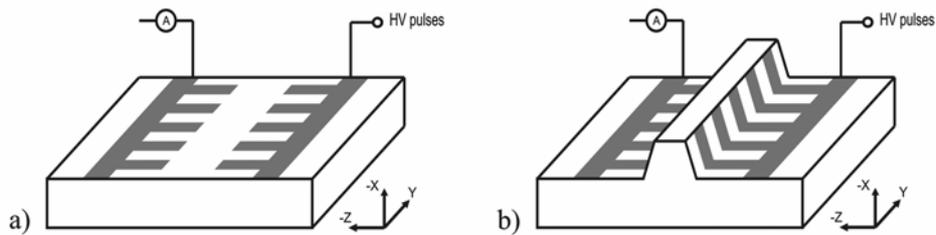**Figure 3** G. Berth et al., Ferroelectrics

Figure 4 G. Berth et al., Ferroelectrics
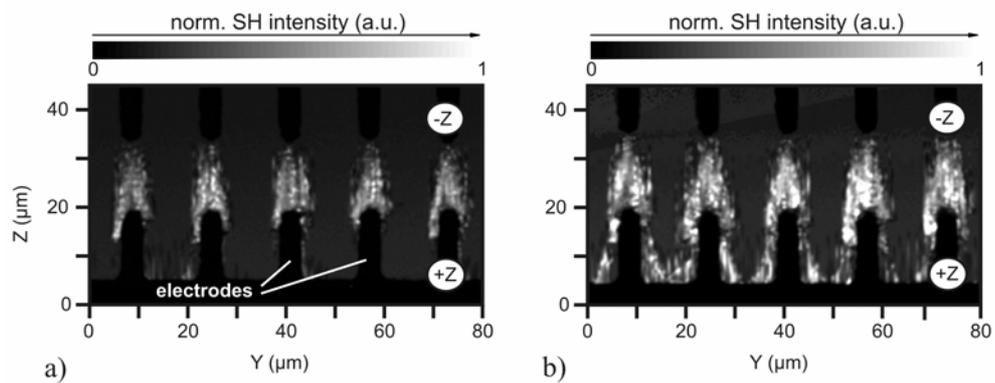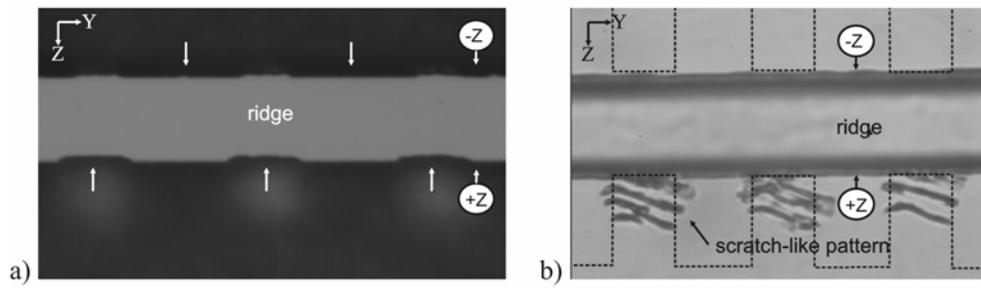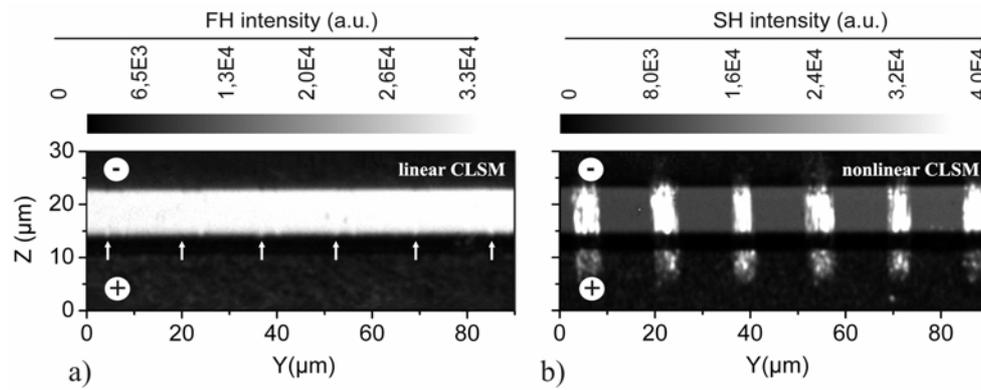
Figure 5 G. Berth et al., Ferroelectrics

Figure 6 G. Berth et al., Ferroelectrics

Figure 7 G. Berth et al., Ferroelectrics
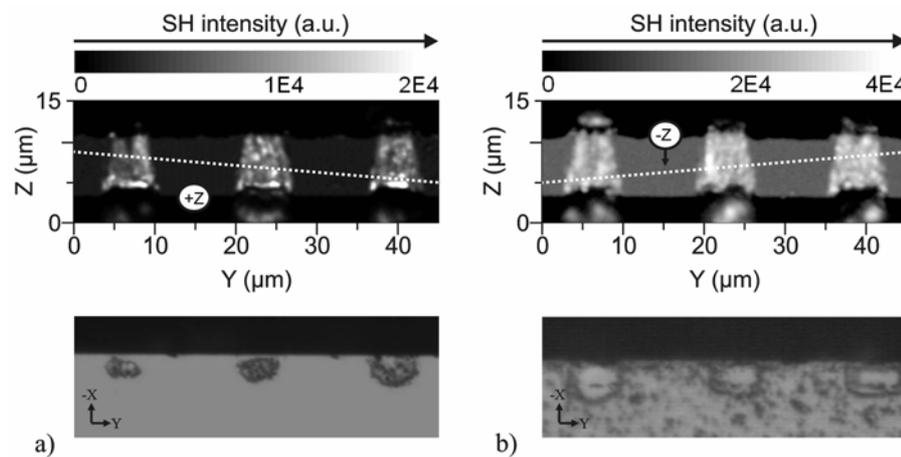

Figure 8 G. Berth et al., Ferroelectrics
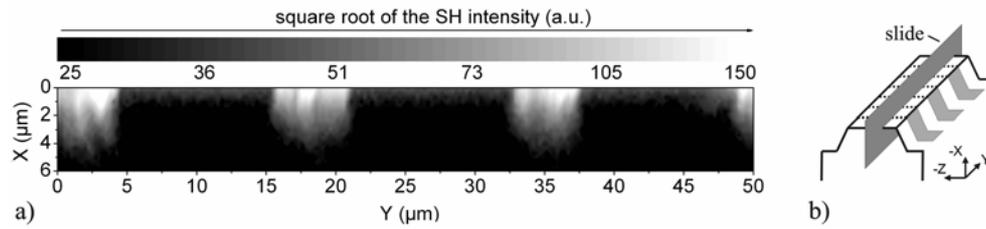
Figure 9 G. Berth et al., Ferroelectrics

a)   b)

Figure 10 G. Berth et al., Ferroelectrics

$(d_x = 0 \ \mu m)$ $(d_x = 1 \ \mu m)$ $(d_x = 2 \ \mu m)$ $(d_x = 3 \ \mu m)$ $(d_x = 4 \ \mu m)$
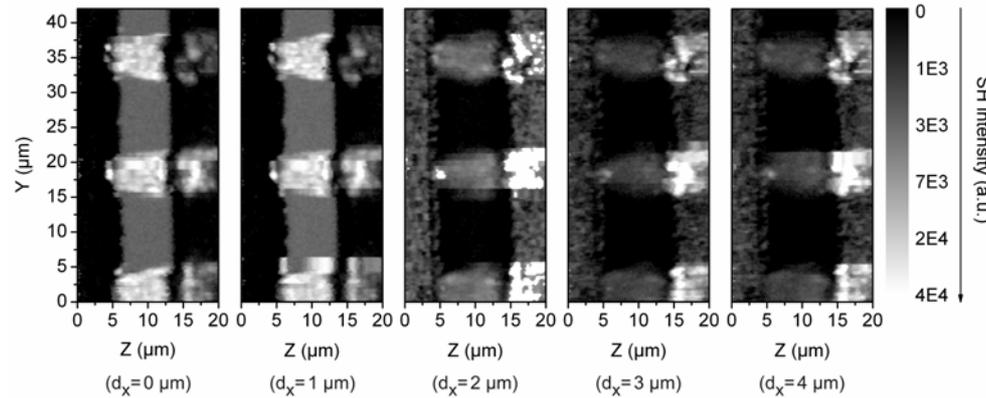
Figure captions:

Figure 1. Schematic of the modular-built confocal microscope.

Figure 2. SEM image of an ICP-etched ridge on X-cut LN (height 3 µm).

Figure 3. Schematic of the poling configuration for a) planar X-cut LN and b) for a ridge on X-cut LN.

Figure 4. SH surface images of periodic micro-domains on planar X-cut LN (scan increment: 250 nm). Poling was performed by 20 rectangular pulses with pulse durations of a) 5 ms and b) 20 ms.

Figure 5. Optical micrographs of a periodically poled ridge on X-cut LN after etching with HF: HNO_3 for 20 minutes without (a) and with (b) scratch-like patterns in the area of removed positive electrodes (dashed lines). The arrows indicate the etched –Z-faces. Note that the focal plane of the microscope coincides with the top (a) and with the bottom (b) of the ridge.

Figure 6. Linear CLSM image (a) and SH microscope image (b) of a periodically poled ridge on X-cut LN taken at the same spatial position (scan increment: 250 nm).

Figure 7. Cross section of a periodically poled ridge on X-cut LN after selective chemical etching. Because of tilted cutting as shown in the inset, cross sections at different positions in Z-direction can be analysed.

Figure 8. Nonlinear confocal surface images of periodically poled ridges on X-cut LN (poled with 5x 5 ms pulses) with a scan increment of 250 nm and corresponding micrographs of the cross sections from similar lines. The samples were poled by a) pulses of 500 V and b) pulses of 550 V. The cutting is indicated by dashed lines.

Figure 9. a) Contour plot of the SH-signal generated inside the ridge by scanning across the domain structure in the X-Y-plane. Scan increment: 250 nm. Here the grey scale represents the square root of SH intensity. b) Schematic of the scan geometry.

Figure 10. Series of nonlinear images generated by scans in the confocal planes of different depths inside the periodically poled ridge. The scan increment in the planes was 250 nm in both lateral directions.

References:

[1] So P. T. C.: Prospects of nonlinear microscopy in the next decade: an overview. Optics Express. 1998; 3: 312-314.

[2] Flörsheimer M., Bösch M., Brillert Ch., Wierschem M., Fuchs H.: Second Harmonic Microscopy – A Quantitative Probe for Molecular Surface Order. Adv. Mater. 1997; 9: 1061-1065.

[3] Uesu Y.: SHG Microscope: Principle and its Applications. Journal of the Korean Physical Society. 1998; 32: 461-463.

[4] Flörsheimer M., Paschotta R., Kubitscheck U., Brillert Ch., Hofmann D., Heuer L., Schreiber G., Verbeek C., Sohler W., Fuchs H.: Second-harmonic imaging of ferroelectric domains in $LiNbO_3$ with micron resolution in lateral and axial directions. Applied Physics B. 1998; 67: 593-599.

[5] Uesu Y., Kurimura S., Yamamoto Y.: NEW NONLINEAR MICROSCOPE AND ITS APPLICATION TO THE OBSERVATION OF FERROELECTRIC DOMAIN STRUCTURE. Ferroelectrics. 1995; 169: 249-257.

[6] Fejer M.M.: Nonlinear Optical Frequency Conversion. Physics Today. 1994; 47: 25.

[7] Myers L. E., Miller G. D., Eckardt R. C., Fejer M. M., Byer R. L., Bosenberg W. R.: Quasi-phase-matched 1.064-mm-pumped optical parametric oscillator in bulk periodically poled $LiNbO_3$. Optics Letters. 1995; 20:1.

[8] Kishino T., Tavlykaeva R. F., Ramaswamy R. V.: 70+ µm deep domain inversion in X-cut $LiNbO_3$ and its use in a high-speed bandpass integrated-optic modulator. Appl. Phys. Lett. 2000; 76: 3852-3854.

[9] Foster M. A., Turner A. C., Lipson M., Gaeta A. L.: Nonlinear Optics in Photonic Nanowires. Optics Express. 2008; 16: 1300-1320.

[10] Berth G., Quiring V., Sohler W., Zrenner A.: Depth-Resolved Analysis of Ferroelectric Domain Strutures in Ti:PPLN Waveguides by Nonlinear Confocal Laser Scanning Microscopy. Ferroelectrics. 2007; 352: 78-85.

[11] Sheppard C. J. R., Shotton D. M.: Confocal Laser Scanning Microscopy. Oxford: IOS Scientific Publishers Ltd.; 1997.

[12] Hu H., Ricken R., Sohler: Etching of Lithium Niobate: From Ridge Waveguides to Photonic Crystal Structures. Conference paper ECIO 2008; WeD3.

[13] Hofmann D.: Nichtlineare, integriert optische Frequenzkonverter für das mittlere Infrarot mit periodisch gepolten Ti:LiNbO$_3$-Streifenwellenleitern. Ph. D.-thesis. University of Paderborn; 2007.

[14] Rosenfeldt A., Flörsheimer M.: Nondestructive remote imaging of ferroelectric domain distributions with high three-dimensional resolution. Applied Physics B. 2001; 73: 523.

[15] Shur V.Y., Batchko R.G., Rumyantsev E.L., Miller G.D., Fejer M.M., Byer R.L.: Domain Engineering: Periodic Domain Patterning in Lithium Niobate. IEEE. 1998; 399-405.